CSIRO
Marine Laboratories

REPORT 89-HC2

HYDROCARBONS IN A LOWER PERMIAN MUDSTONE FROM POATINA, TASMANIA

Prepared by: J.K. Volkman and D.G. Holdsworth
CSIRO Division of Oceanography

Prepared for: Conga Oil Pty. Ltd.
84 Wells Parade
Blackmans Bay
Tasmania

Attention: Mr Malcolm Bendall

May 9th, 1989

SAMPLES

This report presents analytical data for the hydrocarbon composition of a Lower Permian mudstone from Poatina, Tasmania. This sample is thought to be stratigraphically related to the Quamby mudstone (D. Leaman, pers. comm.), which contains *Tasmanites*. The rock sample was provided by Mr Malcolm Bendall of Conga Oil on January 10th., 1989 together with samples of tar from the Midlands. Analytical data for the tar samples are presented in a separate report (Volkman and Holdsworth, 1989).

The sample provided was a single rock fragment. It was grey in colour and had a noticeable petroleum-like smell when broken open. The sample was wire brushed to ensure that no surface contamination was present and crushed using the crushers at the University of Tasmania on January 15th., 1989. 420 grams of crushed sediment were extracted with chloroform to give a yellow-green extract having a strong "oily" smell.

METHODS AND RESULTS

TOTAL LIPID CONTENT

A portion of the chloroform extract was analysed by Iatroscan thin-layer chromatography-flame ionisation detection (Volkman *et al.*, 1986) to determine the total hydrocarbon concentration in the rock. A TLC-FID chromatogram is shown in Figure 1.

Hydrocarbons were the major constituent of the solvent extract and there was only a small amount of polar lipid present. No sterols, alcohols or fatty acids were detectable.

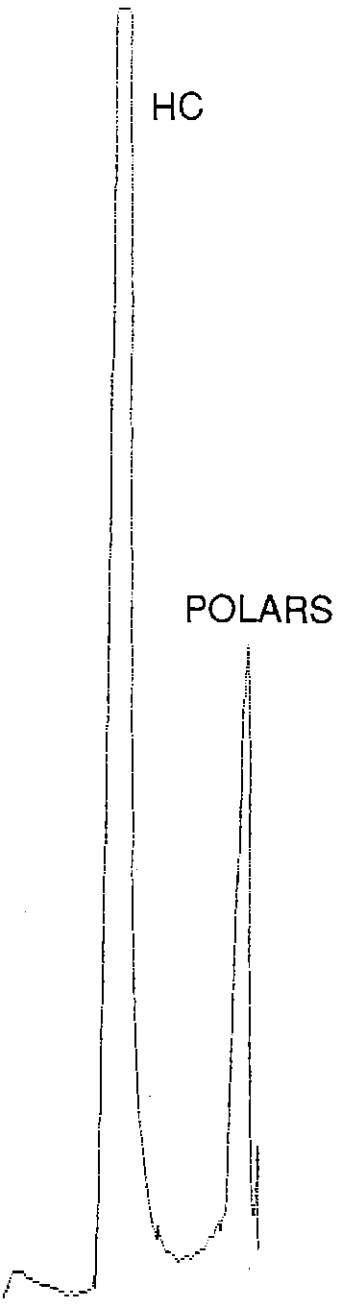

Figure 1. TLC-FID

POLARS-polar lipids

HC- hydrocarbons.

Solvent system: hexane:diethyl ether 94:6.

TABLE 1: CONCENTRATIONS OF HYDROCARBONS AND POLAR COMPOUNDS IN PERMIAN MUDSTONE

HYDROCARBONS	120 μg/g (dry weight)
POLAR COMPOUNDS	4.8 μg/g (dry weight)

The total amount of hydrocarbons is not particularly high, but it must be noted that volatile hydrocarbons (<n-C_{10}) are not be measured by this technique. These are probably quite abundant in this sediment judging from the gas chromatogram of the aliphatic hydrocarbons (Fig. 2).

For comparison, the Permian Inglis siltstone from Oonah has about twice the concentration of extractable hydrocarbons (>n-C_{10}: 270-290 μg/g; Denwer, 1986), and Tasmanite from the same section has 20 times as much (4.25 mg/g; Denwer, 1986).

TOTAL HYDROCARBONS

Total hydrocarbons were separated by applying an aliquot of the total extract to a column of silica gel and eluting with hexane (10 ml) to obtain the aliphatic hydrocarbon fraction. A second fraction containing aromatic hydrocarbons was obtained by eluting with hexane-toluene (10 ml).

Each fraction was analysed by capillary gas chromatography on a 50 meter non-polar methyl silicone fused silica capillary column. A gas chromatogram of the aliphatic hydrocarbons is shown in Figure 2. The distribution of aromatic hydrocarbons is shown in Figure 7.

ALIPHATIC HYDROCARBONS

The aliphatic hydrocarbons show the complete range of homologues that is typical of a mature crude oil. Short-chain (<n-C_{15}) alkanes are particularly abundant, but homologues extended at least to n-C_{36} (Fig. 2). Note that hydrocarbons smaller less than n-C_{10} would have been lost in the extraction procedure.

Branched and cyclic compounds are relatively minor constituents in the gas chromatogram due to the overwhelming predominance of n-alkanes.

The chromatogram also shows a small "unresolved complex mixture" (UCM or hump) throughout the chain-length range. This UCM consists of a very complex mixture of branched and cyclic alkanes that cannot be resolved into individual components, even by the high resolution capillary columns used in this study.

Pristane and phytane are conspicuous constituents in the mudstone (Fig. 2). The pristane/phytane ratio is 2.2; in the Inglis siltstone it is 3.5 (Denwer, 1986). Values greater than 1 are usually associated with an oxic depositional environment.

ALIPHATIC HYDROCARBONS

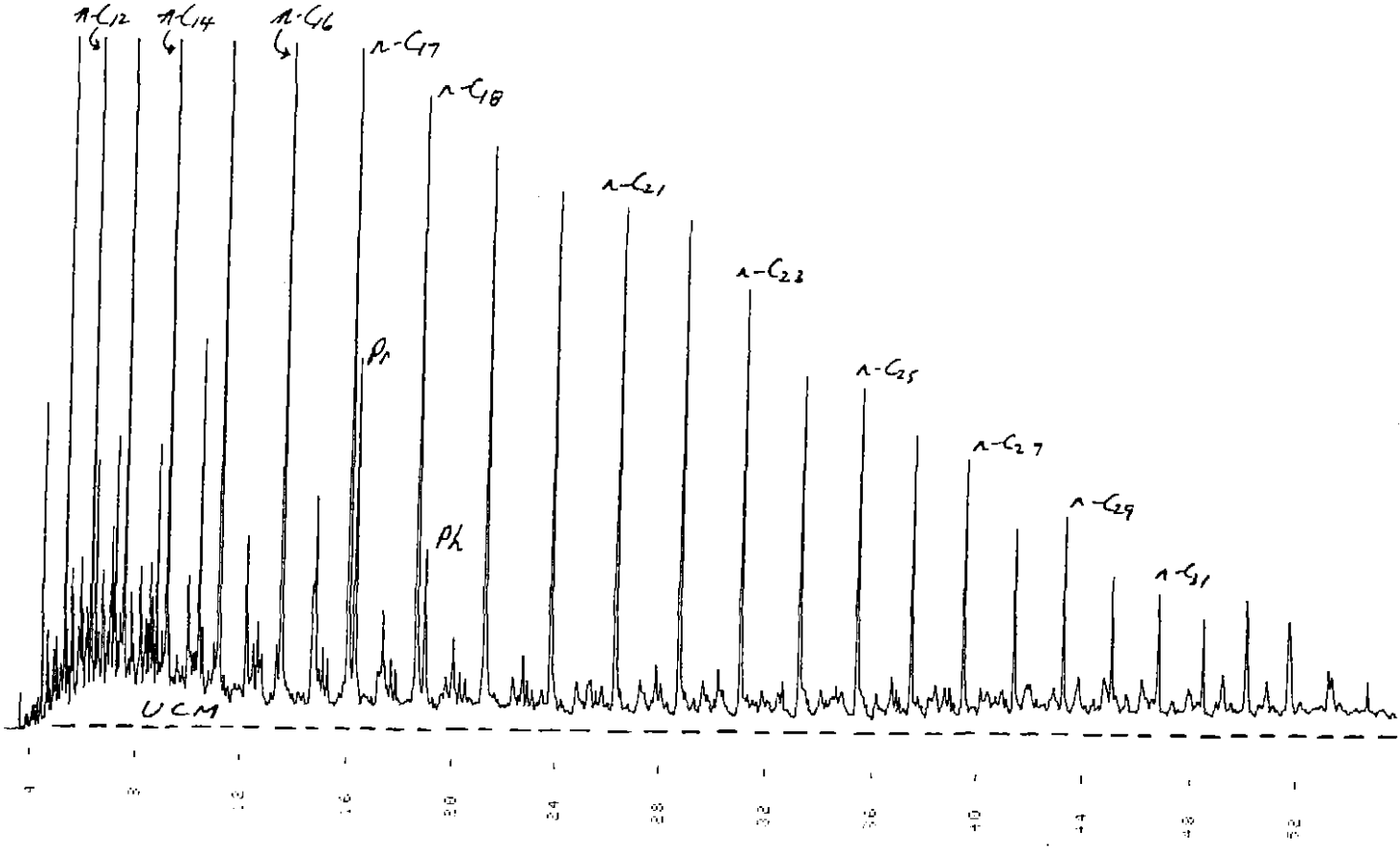

Figure 2. Capillary gas chromatogram of aliphatic hydrocarbons in the mudstone. Pr: pristane; Ph: phytane. n-Alkanes are denoted by n-C_X where "x" is the number of carbon atoms.

BIOMARKERS

To obtain more detailed information about the hydrocarbon composition, the aliphatic hydrocarbon fraction was analysed by gas chromatography-mass spectrometry in selected ion monitoring mode (SIM) and full data acquisition modes.

Distributions of polycyclic biomarkers that are commonly found in crude oils were determined using the selected ion monitoring facility of the mass spectrometer. Data for ions m/z 217 and 218 (steranes), m/z 259 (diasteranes), m/z 191 (hopanes), m/z 177 (demethylated hopanes), m/z 205 (methyl hopanes), m/z 113 and 183 (acyclic isoprenoids) and various molecular ions were acquired.

Tricyclic alkanes

Tricyclic alkanes dominate the m/z 191 mass fragmentograms over most of the carbon-number range (Figure 3), but longer-chain tricyclics are less abundant than hopanes in the higher molecular weight region of the m/z 191 mass fragmentograms (Fig. 4a), as shown by the small peaks eluting between the hopanes.

Tricyclic alkanes are very abundant in Tasmanites (Denwer, 1986; Simoneit *et al.*, 1986), and the distribution is similar to that found in the mudstone (Fig. 3) although the latter contains less of the tricyclic alkanes lower than C_{23}. Isomer ratios also differ probably due to differences in thermal maturity.

Total amounts of tricyclic alkanes in the mudstone are very much less than in Tasmanites. In Tasmanites, the lower molecular weight tricyclic alkanes are more abundant than n-alkanes, but in the mudstone the n-alkanes greatly predominate as shown by the small size of the peaks due to cyclic compounds eluting between the n-alkanes (Fig. 2).

Hopanes

Hopane distributions as represented by mass fragmentograms of the major fragment ion m/z 191 are shown in Figure 3 and 4a (C_{26}-C_{36} hopane range).

The hopane distribution in the mudstone is quite distinctive with a high predominance of the C_{30} hopane (peak H5; Fig. 4a), and comparatively low abundance of extended (>C_{30}) hopanes. The C_{29} hopane (peak H3) is surprisingly low in abundance. Hopanes having an "immature" ββ stereochemistry and unsaturated hopenes were not detected. Moretanes (peaks H4 and H5) are present in very minor amounts.

Hopane distributions can be used to ascertain the degree of thermal maturity from the relative proportions of key isomers.

(a) In the extended hopanes (i.e. >C_{30}) the 22S epimer is more abundant than the 22R epimer (e.g. peaks H7 and H8) which is typical of mature sediments. These isomers isomerise to an equilibrium mixture at maturities before the oil window.

(b) Moretanes (peaks H4 and H6) are very minor components compared with 17α(H),21β(H)-hopanes of the same chain-length (peaks H3 and H5). Similar ratios are found in mature crude oils.

Key 1. Identifications of peaks in hopane (m/z 191) and methyl hopane (m/z 205) mass fragmentograms

PEAK		COMPOUND
H1	C_{27}	18α(H)-22,29,30-trisnorneohopane (Ts)
H2	C_{27}	17α(H)-22,29,30-trisnorhopane (Tm)
H3	C_{29}	17α(H),21ß(H)-30-norhopane
H4	C_{29}	17ß(H),21α(H)-30-normoretane
H5	C_{30}	17α(H),21ß(H)-hopane
H6	C_{30}	17ß(H),21α(H)-moretane
H7	C_{31}	(22S)-17α(H),21ß(H)-homohopane
H8	C_{31}	(22R)-17α(H),21ß(H)-homohopane
H9	C_{32}	(22S)-17α(H),21ß(H)-bishomohopane
H10	C_{32}	(22R)-17α(H),21ß(H)-bishomohopane
H11	C_{33}	(22S)-17α(H),21ß(H)-trishomohopane
H12	C_{33}	(22R)-17α(H),21ß(H)-trishomohopane
H13	C_{34}	(22S)-17α(H),21ß(H)-tetrakishomohopane
H14	C_{34}	(22R)-17α(H),21ß(H)-tetrakishomohopane
H15	C_{35}	(22S)-17α(H),21ß(H)-pentakishomohopane
H16	C_{35}	(22R)-17α(H),21ß(H)-pentakishomohopane
M1	C_{28}	18α(H)-2-methyl-22,29,30-trisnorneohopane
M2	C_{28}	17α(H)-2-methyl-22,29,30-trisnorhopane
M3	C_{30}	17α(H),21ß(H)-2-methyl-30-norhopane
M4	C_{30}	17ß(H),21α(H)-2-methyl-30-normoretane
M5	C_{31}	17α(H),21ß(H)-2-methylhopane
M6	C_{31}	17ß(H),21α(H)-2-methylmoretane
M7	C_{32}	(22S)-17α(H),21ß(H)-2-methylhomohopane
M8	C_{32}	(22R)-17α(H),21ß(H)-2-methylhomohopane
M9	C_{33}	(22S)-17α(H),21ß(H)-2-methylbishomohopane
M10	C_{33}	(22R)-17α(H),21ß(H)-2-methylbishomohopane
M11	C_{34}	(22S)-17α(H),21ß(H)-2-methyltrishomohopane
M12	C_{34}	(22R)-17α(H),21ß(H)-2-methyltrishomohopane
M13	C_{35}	(22S)-17α(H),21ß(H)-2-methyltetrakishomohopane
M14	C_{35}	(22R)-17α(H),21ß(H)-2-methyltetrakishomohopane
M15	C_{36}	(22S)-17α(H),21ß(H)-2-methylpentakishomohopane
M16	C_{36}	(22R)-17α(H),21ß(H)-2-methylpentakishomohopane

Key 2. Identifications of peaks in sterane and diasterane (m/z 217 and 218) mass fragmentograms.

PEAK		COMPOUND
S1	C_{27}	(20S)-5α(H),14α(H),17α(H)-cholestane
S2	C_{27}	(20R)-5α(H),14ß(H),17ß(H)-cholestane
S3	C_{27}	(20S)-5α(H),14ß(H),17ß(H)-cholestane
S4	C_{27}	(20R)-5α(H),14α(H),17α(H)-cholestane
S5	C_{28}	(20S)-5α(H),14α(H),17α(H)-24-methylcholestane
S6	C_{28}	(20R)-5α(H),14ß(H),17ß(H)-24-methylcholestane
S7	C_{28}	(20S)-5α(H),14ß(H),17ß(H)-24-methylcholestane
S8	C_{28}	(20R)-5α(H),14α(H),17α(H)-24-methylcholestane
S9	C_{29}	(20S)-5α(H),14α(H),17α(H)-24-ethylcholestane
S10	C_{29}	(20R)-5α(H),14ß(H),17ß(H)-24-ethylcholestane
S11	C_{29}	(20S)-5α(H),14ß(H),17ß(H)-24-ethylcholestane
S12	C_{29}	(20R)-5α(H),14α(H),17α(H)-24-ethylcholestane
D1	C_{27}	(20S)-13ß(H),17α(H)-diasterane
D2	C_{27}	(20R)-13ß(H),17α(H)-diasterane
D3	C_{29}	(20S)-13ß(H),17α(H)-diasterane
D4	C_{29}	(20R)-13ß(H),17α(H)-diasterane

TRICYCLIC HYDROCARBONS AND HOPANES

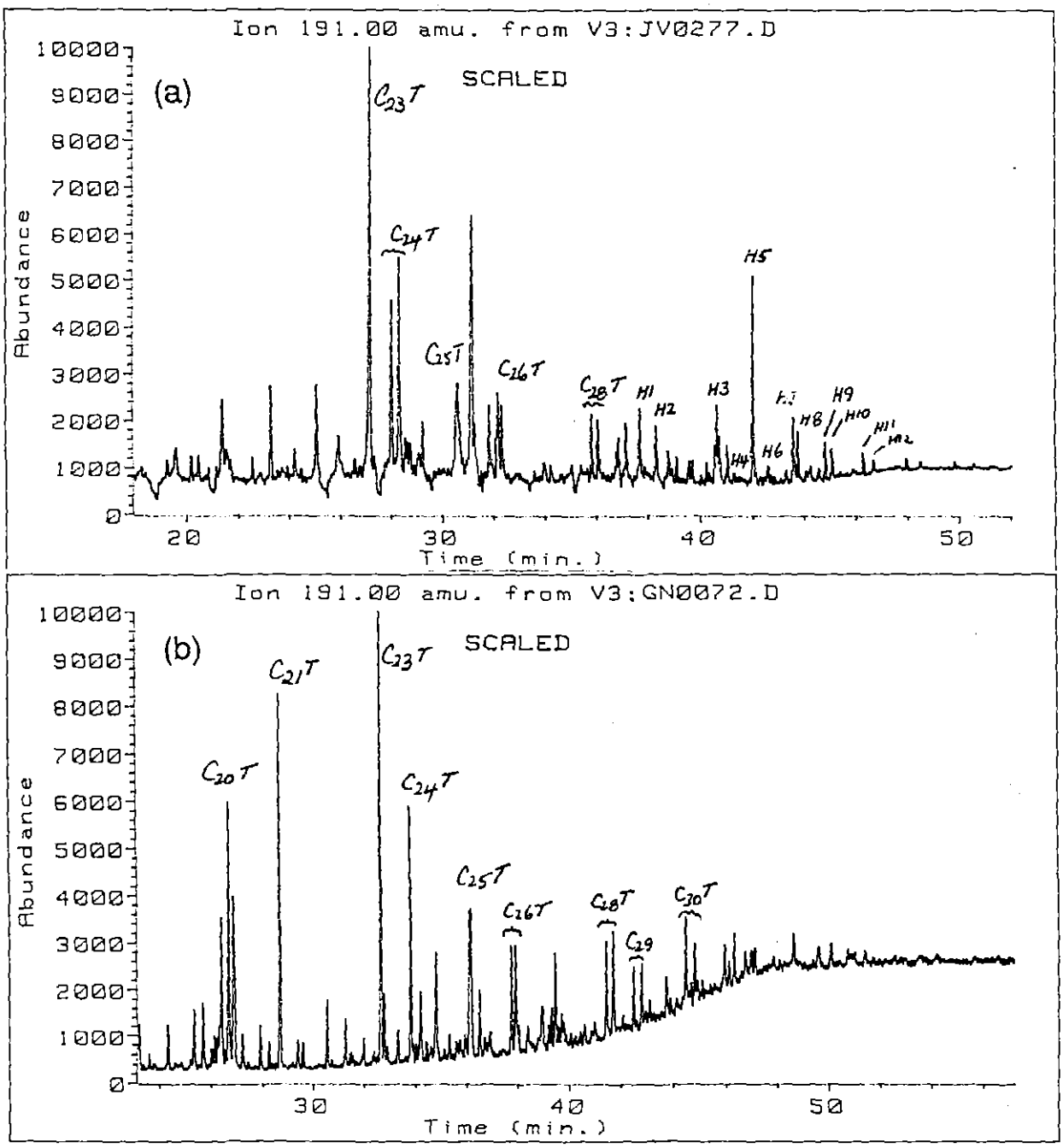

Figure 3. Mass fragmentograms for m/z 191 in (a) Permian mudstone and (b) Tasmanite. Tricyclic alkanes are denoted by C_xT where "x" is the number of carbon atoms. Note the general similarities of the tricyclic alkane distributions and higher relative abundance of hopanes (labelled H) in the mudstone. The mudstone has much smaller amounts of C_{20} and C_{21} tricyclic alkanes than Tasmanite.

HOPANES AND METHYL HOPANES

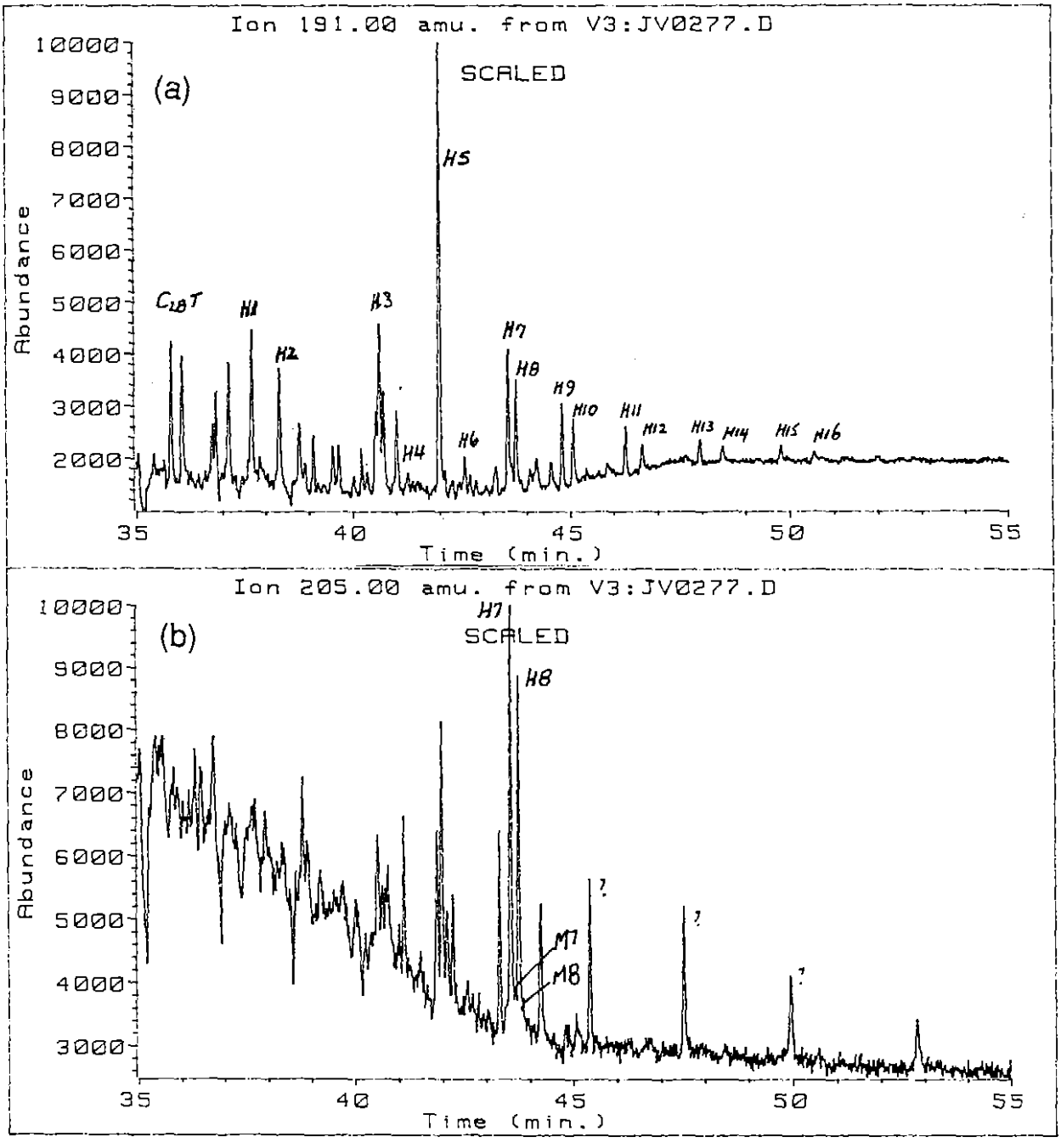

Figure 4. Mass fragmentograms for (a) m/z 191 and (b) m/z 205 showing distributions of hopanes (labelled H) and methyl hopanes (labelled M). See accompanying Key 1 for peak identifications. Note the lack of significant amounts of methyl hopanes. Tricyclic alkanes are denoted by T.

(c) The ratio of the two C_{27} hopanes Ts (peak H1) and Tm (peak H2) is a sensitive indicator of thermal maturity. Ts is almost as abundant as Tm indicating that these hydrocarbons were produced at a high thermal maturity. The equivalent vitrinite reflectance would be in excess of 0.7.

The hopane distributions are very different from those found in suspected seep samples from Bruny Island (Volkman, 1987) or in Ordovician carbonates from Queenstown and Ida Bay (Volkman, 1988). The hopane distributions of the latter contain the C_{29} hopane as a major component, and extended hopanes are relatively more abundant.

Demethylated hopanes

A m/z 177 mass fragmentogram (data not shown), showed that demethylated hopanes were not present in the mudstone. These are commonly associated with highly biodegraded residues of crude oil (Volkman *et al.*, 1983).

Methyl hopanes

The mudstone contains only trace amounts of 2-methyl hopanes as shown by the m/z 205 mass fragmentogram (Fig. 4b). Methyl hopanes are abundant in the Ordovician carbonates (Volkman, 1988), and in most oils derived from carbonate source rocks although they are not restricted to this source facies.

Steranes

Distributions of steranes can provide information about the maturity and source of a crude oil. Mass fragmentograms for m/z 217 and m/z 218 are shown in Figure 5.

C_{27} steranes are only slightly more abundant than C_{29} steranes; C_{28} steranes are also present in moderate amounts (Fig. 5). Sterane maturity parameters are consistent with a fairly high maturity which is consistent with the hopane parameters. Note the higher abundance of ∝ßß isomers (peaks S10 and S11) compared with ααα isomers (peaks S9 and S12) (Fig. 5).

C_{27} and C_{29} diasteranes (rearranged steranes) are very abundant (peaks labelled D in Fig. 5). Diasteranes are typically abundant where the source rocks contain large amounts of clays which catalyse the steroid backbone rearrangement.

The m/z 217 mass fragmentogram over the entire carbon number range shows an abundance of lower molecular weight steranes (Fig. 6). Individual components have not been identified, but such compounds are usually associated with thermal cracking of higher molecular weight steranes and diasteranes in oils of higher maturity.

Steranes in Tasmanites show a much higher predominance of C_{29} components and the diasterane/sterane ratio is much less than in the mudstone (Denwer, 1986).

STERANES AND DIASTERANES

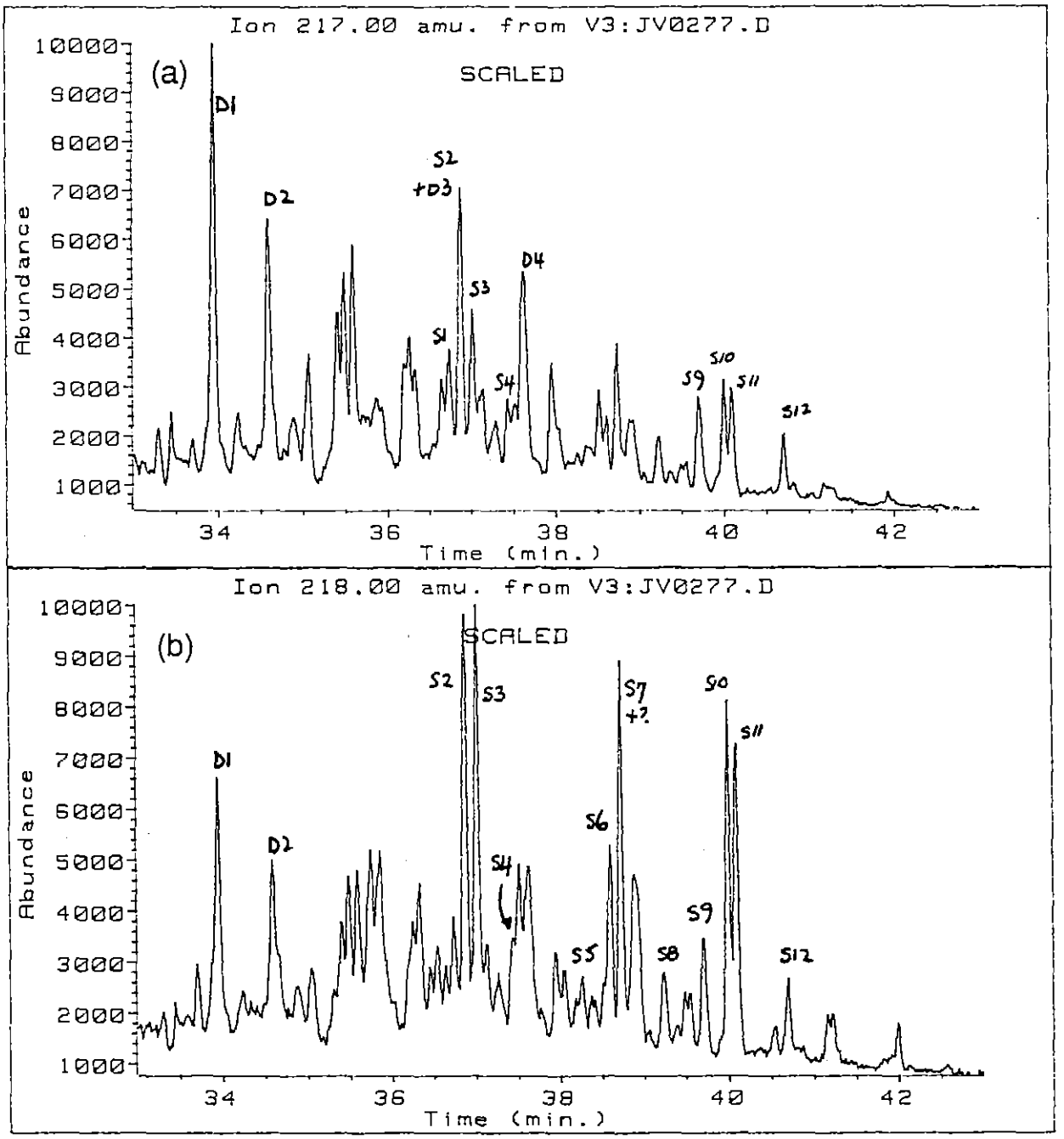

Figure 5. Mass fragmentograms for (a) m/z 217 and (b) m/z 218 showing distribution of C_{26}-C_{30} steranes (labelled S) and diasteranes (labelled D). See accompanying Key 2 for peak identifications. Note the high abundance of diasteranes which is often associated with sediments containing a high clay content.

STERANES AND DIASTERANES

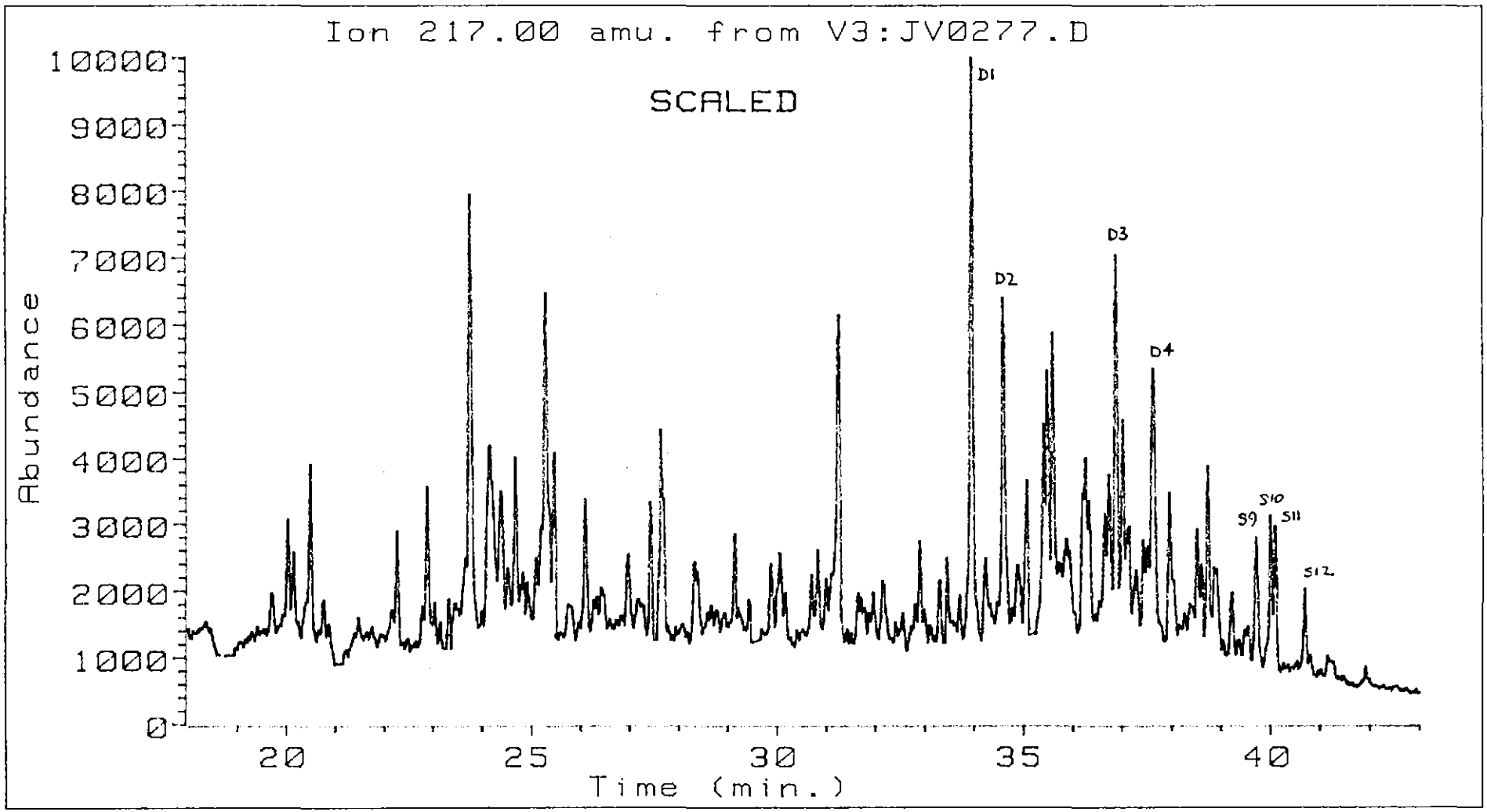

Figure 6. Mass fragmentogram for m/z 217 showing the distribution of C_{20}-C_{30} steranes and diasteranes. See accompanying Key 2 for peak identifications. Note the high abundance of shorter-chain steranes (isomers not identified).

AROMATIC HYDROCARBONS

A preliminary investigation was carried out on the aromatic hydrocarbon fraction since the extract had a distinctly "aromatic" smell. A capillary gas chromatogram of the total aromatic hydrocarbon fraction is shown in Fig. 7. Analysis by capillary gas chromatography-mass spectrometry in full scan and selected ion monitoring modes was used to identify major constituents.

The aromatic fraction contains an abundance of low molecular weight components (mainly alkyl naphthalenes) which is typical of a mature crude oil. Naphthalene and more volatile aromatic hydrocarbons would have been lost in the extraction procedures.

Distributions of methyl naphthalenes, dimethyl naphthalenes, and trimethyl naphthalenes are shown in Fig. 8 as mass fragmentograms of the corresponding molecular ions (m/z 142, 156 and 170 respectively).

Phenanthrene and alkyl phenanthrenes are less abundant, but still represent significant components of the aromatic fraction. Distributions of phenanthrene, methyl phenanthrenes and dimethyl phenanthrenes are shown in Fig. 9 as mass fragmentograms of the corresponding molecular ions (m/z 178, 192 and 206 respectively).

The methyl phenanthrene index calculated from the abundance of phenanthrene and methyl phenanthrene isomers according to Radke *et al.* (1983) was 0.66 corresponding to a vitrinite reflectance of about 0.75. This value must be treated with some caution, but it usually gives a reasonable indication of the degree of thermal maturation to which the source rock has been subjected.

The aromatic hydrocarbon fraction contains a major compound eluting at 32 minutes (Fig. 7). The mass spectrum is shown in Fig. 10b. A mass fragmentogram for the base peak m/z 159 (Fig. 11) showed that this compound was not part of a series, but a related compound with a base peak at m/z 145 was also detected in small amounts. A mass spectrum is shown in Fig. 10a. The identity of these compounds has not been established but they may be aromatic sulphur compounds.

Aromatic steroid hydrocarbons were present in very small amounts. Mass fragmentograms for m/z 231 (triaromatic sterids) and m/z 253 (monoaromatic steroids) are shown in Fig. 12. Both distributions are dominated by shorter-chain components which lack the side-chains of the parent sterols due to thermal cracking reactions. Such distributions are typical of mature crude oils.

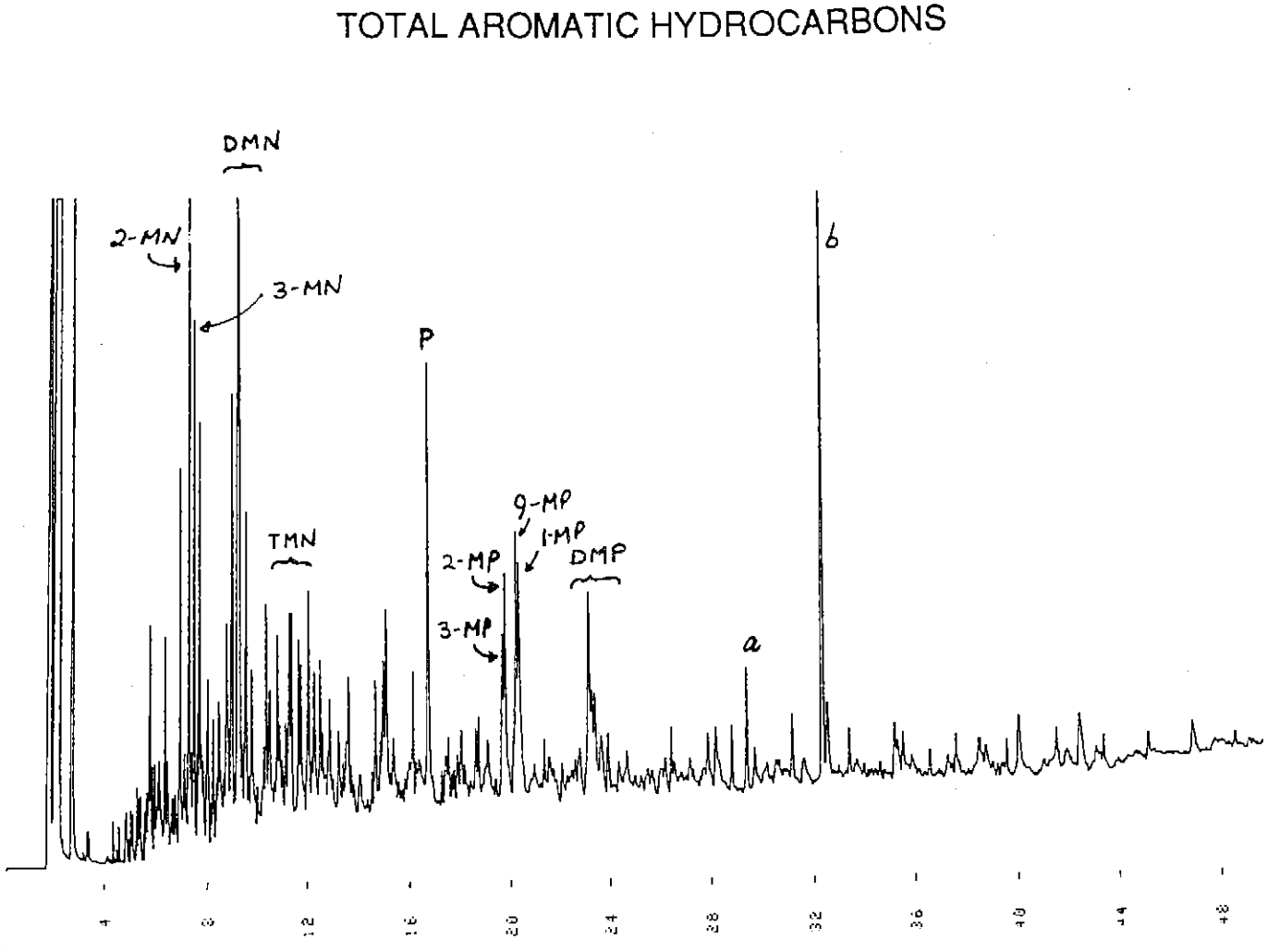

Figure 7. Capillary gas chromatogram showing the distribution of aromatic hydrocarbons. MN: methyl naphthalenes, DMN: dimethyl naphthalenes, TMN: trimethyl naphthalenes; P: phenanthrene, MP: methyl phenanthrenes, DMP: dimethyl phenanthrenes. Peaks a and b are unknown (see text; mass spectra are shown in Fig. 10).

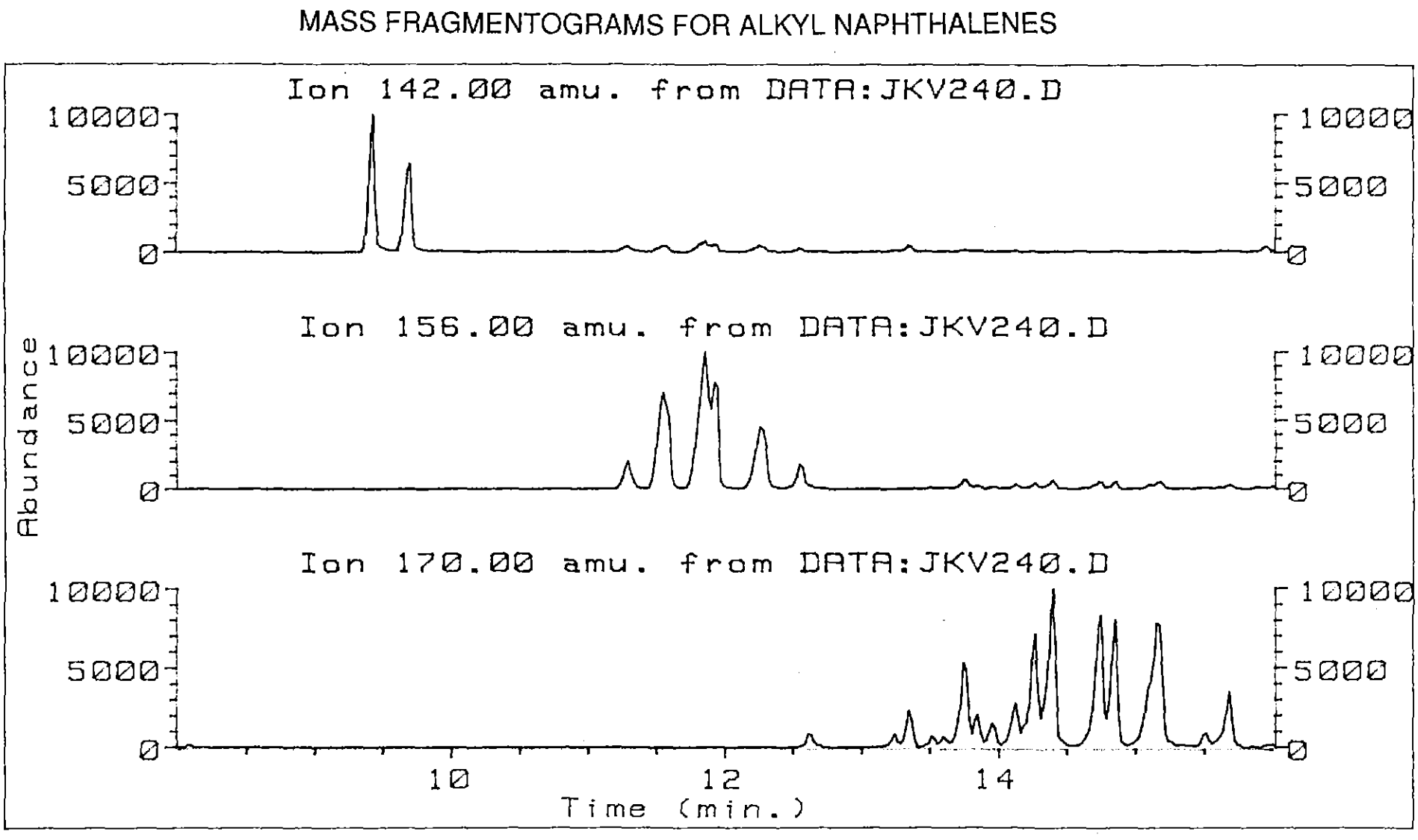

Figure 8. Mass fragmentograms for m/z 142 (*methyl naphthalenes*), m/z 156 (dimethyl naphthalenes) and m/z 170 (trimethyl naphthalenes).

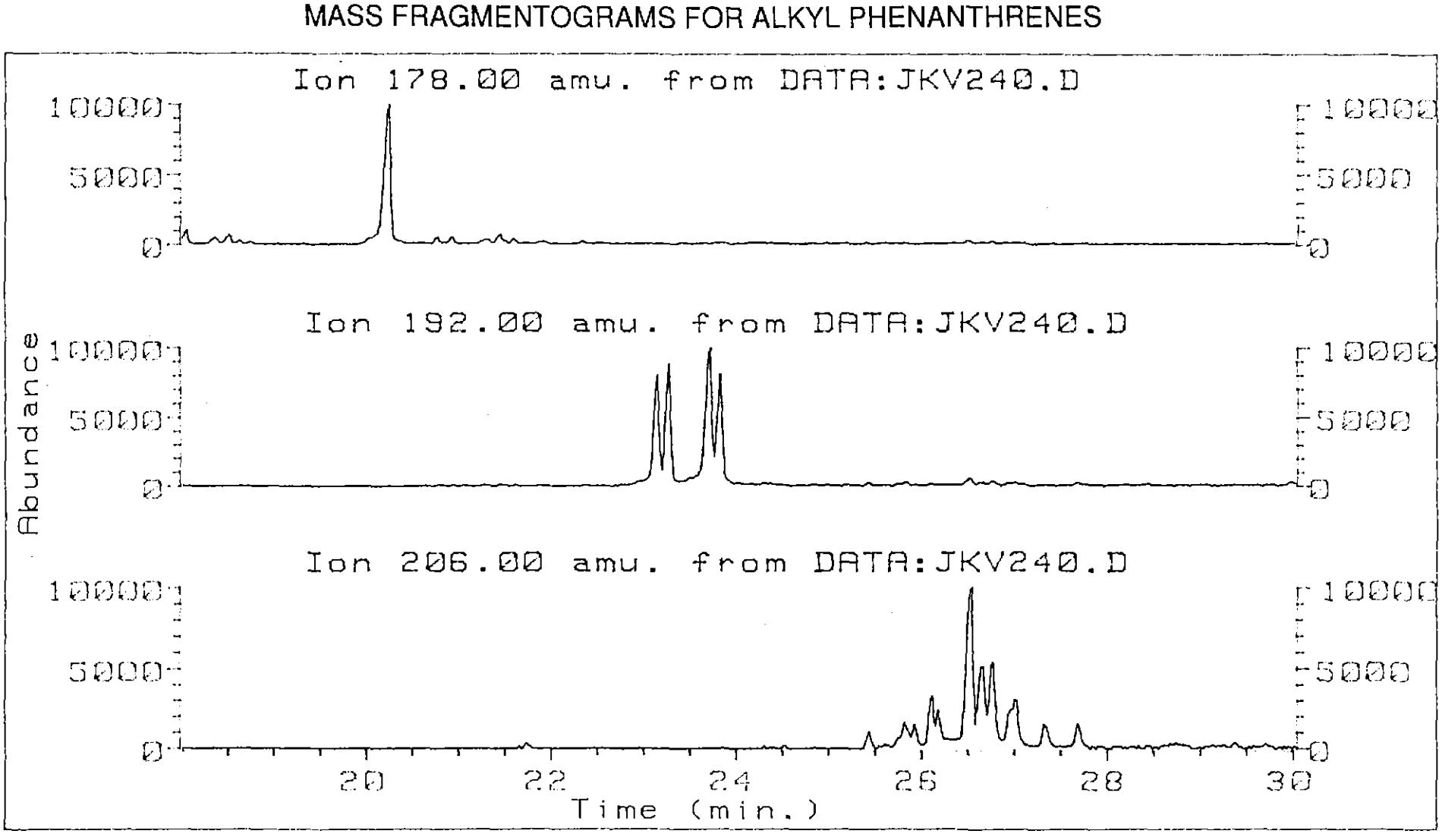

Figure 9. Mass fragmentograms for m/z 178 (phenanthrene), m/z 192 (methyl phenanthrenes) and m/z 206 (dimethyl phenanthrenes).

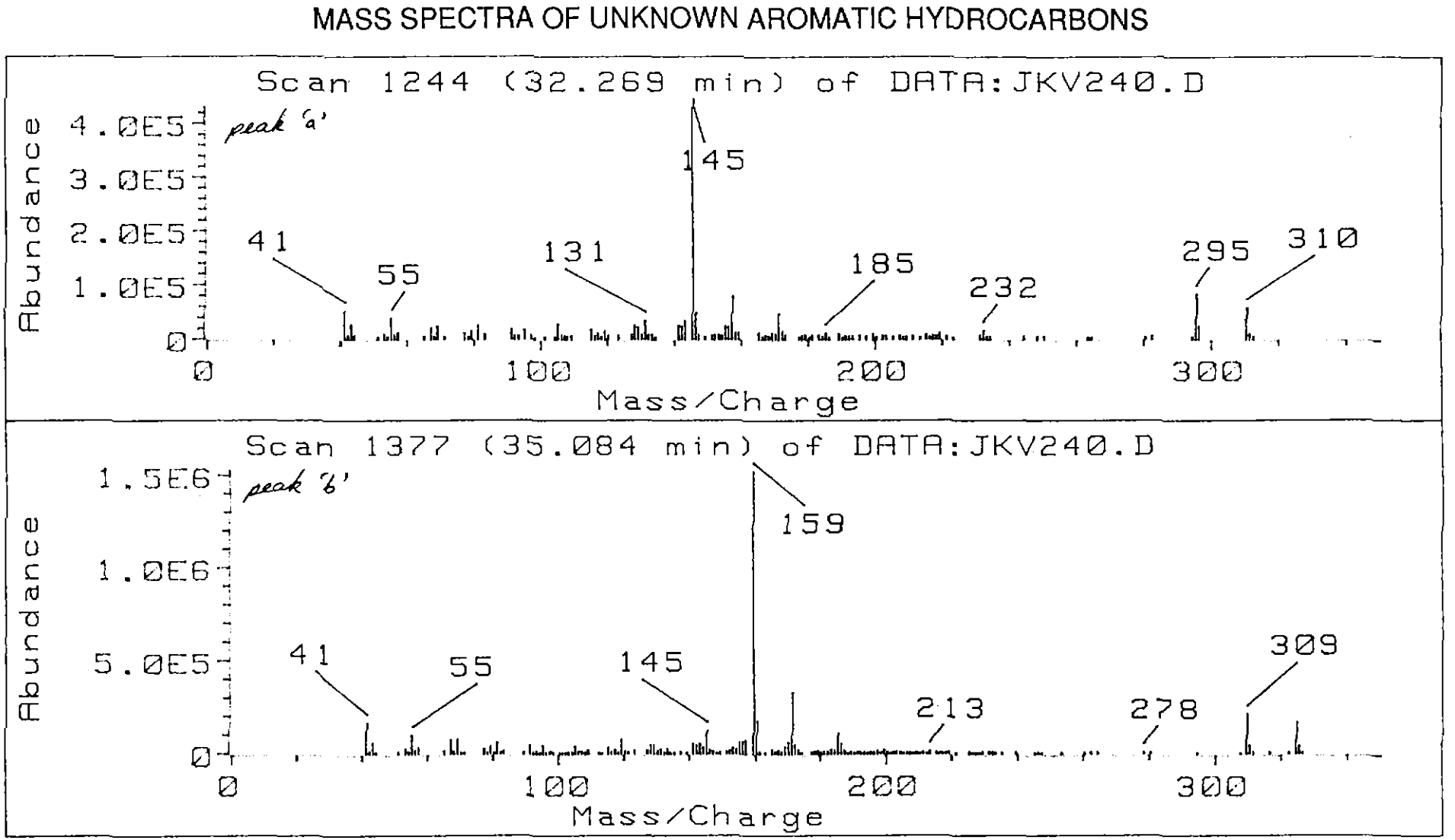

Figure 10. Mass spectra of two unknown compounds in the aromatic hydrocarbon fraction.

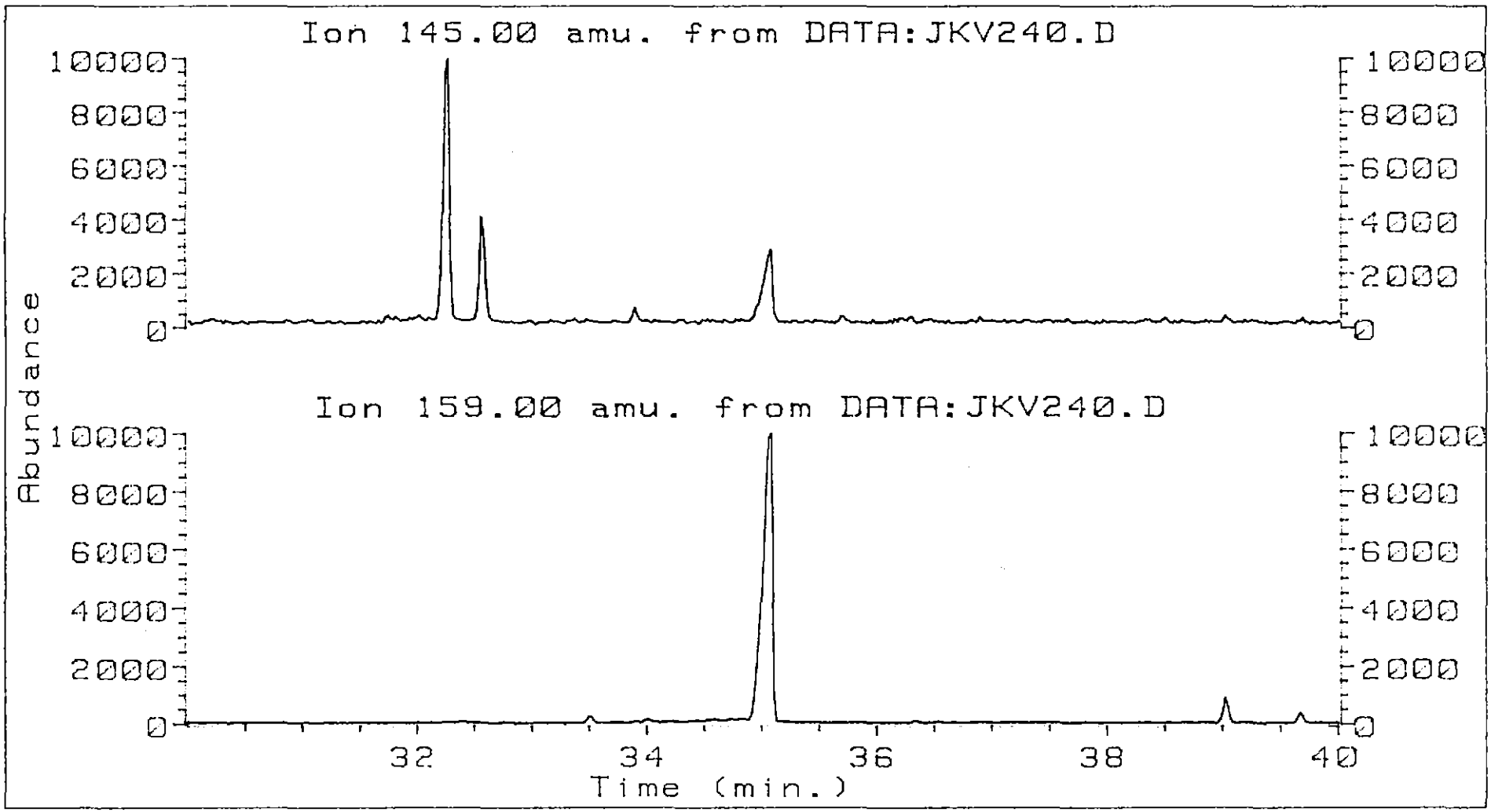

Figure 11. Mass fragmentograms for m/z 145 and m/z 159 showing distribution of unknown compounds in the aromatic fraction.

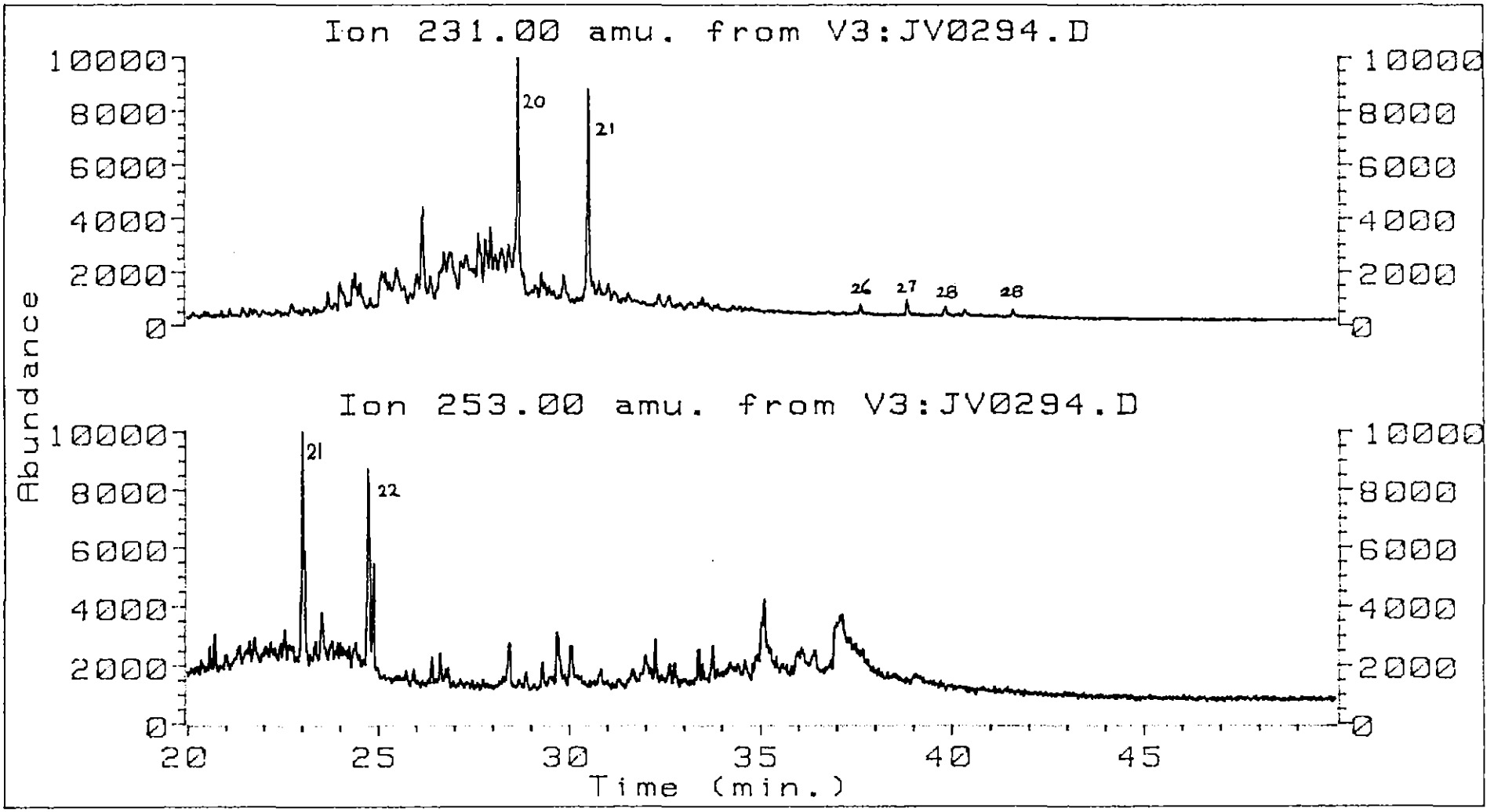

Figure 12. Mass fragmentograms for m/z 231 and m/z 253 showing distribution of triaromatic and monoaromatic steroid hydrocarbons respectively. Numerals indicate the total number of carbon atoms.

CONCLUSIONS

The mudstone contains appreciable amounts of hydrocarbons having the characteristic distributions found in a mature crude oil. n-Alkanes and low molecular weight aromatic hydrocarbons are abundant constituents which is typical of petroleum.

The biomarker distributions are distinctly different from those found in Ordovician carbonates. Methyl hopanes are very minor constituents and diasteranes (which are commonly associated with sediments containing a high content of clays) are abundant.

The total amount of extractable hydrocarbons determined by TLC-FID is at least 120 ppm. This value is likely to be a significant underestimate due to losses of volatile components in the extraction steps.

The methyl phenanthrene ratio suggest that the hydrocarbons were generated at a thermal maturity equivalent to a vitrinite relectance of about 0.75 i.e. well into the oil window. Aliphatic biomarker parameters suggest a similar level of maturity.

The presence of tricylic alkanes suggest that *Tasmanites* may have been the source of some of the hydrocarbons, but their low abundance relative to n-alkanes indicates that other sources are probably more important.

These data do not exclude the possibility that the hydrocarbons have migrated into the rock rather than the result of *in situ* production. However, there was no sign of staining and the general similarity of the distributions to those in stratigraphically related Inglis siltstone suggest that they are indigenous to the rock.

I recommend that if further studies are considered then a high priority be given to obtaining Rock Eval data to assess the source potential of the mudstone. It would also be of interest to identify whether *Tasmanites* was present from microscopic examination.

REFERENCES

Denwer, K. (1986) Geology and geochemistry of the tasmanite oil shale. B. Sc (Hons) Thesis, Geology Department, University of Tasmania. 84 pp.

Simoneit, B.R.T., J.O. Grimalt, T.G. Wang, R.E. Cox, P.G. Hatcher and A. Nissenbaum (1986) Cyclic terpenoids of contemporary resinous plant detritus and of fossil woods, ambers and coals. *Organic Geochemistry* **10**, 877-889.

Volkman J. K., R. Alexander, R. I. Kagi, and G. W. Woodhouse (1983). Demethylated hopanes in crude oils and their applications in petroleum geochemistry. *Geochim. Cosmochim. Acta.* **47**, 785-794.

Volkman, J.K., D. A. Everitt and D. I. Allen (1986) Some analyses of lipid classes in marine organisms, sediments and seawater using thin-layer chromatography-flame ionisation detection. *J. Chromatogr.* **356**, 147-162.

Volkman, J.K. (1987) Analysis of sediment and water samples from Bruny Island for petroleum hydrocarbons. Report 87-HC2 to Conga Oil.

Volkman, J.K. (1988) Hydrocarbons in Ordovician limestones from Queenstown and Lune River, Tasmania. Report 88-HC1 to Conga Oil.

Volkman, J.K. and D.G. Holdsworth (1989) Hydrocarbons in two tar samples from the Midlands, Tasmania. Report 89-HC1 to Conga Oil.